Journal of Materials Chemistry A

Efficient Hydrogen Evolution Reaction by Molybdenum Carbide and Molybdenum Nitride Nanocatalysts Synthesized via a Urea Glass Route

Journal:	*Journal of Materials Chemistry A*
Manuscript ID:	TA-ART-01-2015-000139.R2
Article Type:	Paper
Date Submitted by the Author:	28-Feb-2015

Complete List of Authors:	Ma, Liang; National University of Singapore, Chemistry Ting, Rui Ling Louisa; National University of Singapore, Chemistry Molinari, Valerio; Max-Planck-Institute of Colloids and Interfaces, Department of Colloid Chemistry Giordano, Cristina; Max-Planck-Institute of Colloids and Interfaces, Department of Colloid Chemistry Yeo, Boon Siang; National University of Singapore, Department of Chemistry

Efficient Hydrogen Evolution Reaction by Molybdenum Carbide and Molybdenum Nitride Nanocatalysts Synthesized via a Urea Glass Route

Liang Ma[1], Rui Lin Louisa Ting[1], Valerio Molinari[2], Cristina Giordano[2], Boon Siang Yeo[1,*]

[1] Department of Chemistry, National University of Singapore, 3 Science Drive 3, Singapore 117543

[2] Max-Planck-Institute of Colloids and Interfaces, Department of Colloid Chemistry, Research Campus Golm, D-14424 Potsdam, Germany

*Author to whom correspondence should be addressed: chmyeos@nus.edu.sg, Fax: +65 6779 1691, Tel: +65 6516 2836

Abstract

Molybdenum carbide and molybdenum nitride nanoparticles have been developed for catalyzing the hydrogen evolution reaction (HER). These nanocatalysts were synthesized by the 'urea glass route'. By simply changing the molar ratio of the urea/metal precursor, α-Mo_2C and γ-Mo_2N nanoparticles, both of which are crystalline, phase pure and monodisperse in size, were obtained. Hydrogen evolution was performed in both 1M KOH and 0.5M H_2SO_4 electrolytes, and characterized by linear sweep voltammetry and electrochemical impedance spectroscopy. The as-synthesized Mo_2C showed excellent HER performance especially in KOH. At a catalyst loading of 102 μg cm^{-2}, a low overpotential of 176 mV was needed to produce 10 mA cm^{-2} of H_2. Its measured currents and turnover frequencies for hydrogen evolution at different overpotentials compare favorably against many other recently-reported non-precious metal HER catalysts. Online gas chromatography demonstrated that the current efficiency for H_2 production is ~100%. Both Mo_2C and Mo_2N showed negligible overpotential losses after acceleration degradation tests in acid and alkali. This is noteworthy since very few catalysts are active in these two extreme pHs. An attractive aspect of the α-Mo_2C or γ-Mo_2N nanoparticles for electrochemical hydrogen evolution is that they are simple and well-characterized in chemical and physical composition. The excellent catalytic activity of the α-Mo_2C catalysts is attributed to its small particle size which will facilitate a rapid electron transfer for the hydrogen evolution reaction. Our study placed the as-synthesized α-Mo_2C nanoparticles as highly promising alternatives for platinum in the alkaline water electrolyzer.

Keywords:

Hydrogen evolution reaction, electrocatalysis, molybdenum compounds, water splitting, electrochemistry.

1. Introduction

The electrolysis of water using solar electricity is a sustainable and environmental-friendly method for producing hydrogen gas (H_2) fuel.[1-3] Water can be reduced to H_2 in acid or alkali via respectively the half reactions $2H^+ + 2e^- \rightarrow H_2$ or $2H_2O + 2e^- \rightarrow 2OH^- + H_2$ (the hydrogen evolution reaction, HER). The HER is most effectively catalyzed by platinum.[4, 5] The scarcity and high cost of platinum, however, limit its use on the industrial scale. Thus, commercial alkaline electrolyzers typically employ cheaper but inferior alternatives such as nickel and its alloys. To bridge the gap between economic feasibility and catalyst efficiency, extensive efforts have been devoted over the years to develop efficacious HER catalysts based on earth-abundant materials. Among these alternatives, molybdenum carbides (Mo_2C) and molybdenum nitrides (Mo_2N) possess catalytic and electronic properties which resemble that of platinum, and has therefore been identified as promising materials for catalyzing the HER.[3, 6-16]

A wide range of HER catalytic activities by both bulk and nanostructured Mo_2C and Mo_2N has been observed, mainly in acidic electrolytes.[3, 6-16] The efficacy of these materials in electroreducing water is inferior to Pt, and is highly dependent on their surface composition and structure. Mo_2C is generally more active than Mo_2N. These two compounds are usually synthesized by chemical vapor deposition (CVD), nitridation of Mo oxides and/or pyrolysis of organo Mo complexes.[17-19] During or after their preparation, they can also be attached onto supports to enhance their catalytic activities. For example, Mo_2C anchored onto carbon nanotubes show superior electrocatalytic activity and stability towards HER compared to bulk Mo_2C.[7, 10] The electroactivity of Mo nitride for HER has also been significantly improved by incorporating Ni and Co into its lattice structure.[8, 9] Existing synthetic methods for Mo_2C and Mo_2N, however, often produce catalysts that have heterogeneous structures, low crystallinity,

and are polydisperse in sizes and composition.[11, 20] Furthermore, amorphous carbon produced from the pyrolysis of carbonaceous gases during CVD can cover and deactivate the catalytic active sites.[11, 21, 22]

These limitations could be overcome by preparing Mo_2C and Mo_2N nanoparticles via a simple 'urea glass' route, previously set up in our lab.[23] The advantage of this method is the ability to produce nanoparticles with the much-required crystallinity, purity and monodisperse size.[20, 24] In this route, urea plays the dual role of C/N source and stabilizing agent during the necessary heat treatment to convert the precursor mixtures into the desired metal carbide or metal nitride, with none or negligible residual amount of C (in the nitride phase) or N (in the carbide phase).[23] Using a modification of our method, Mo_2C and Mo_2N nanoparticles anchored on carbon nanotube-graphene supports were recently found to be active for HER in 0.5 M H_2SO_4.[25]

We contribute here an investigation of hydrogen evolution catalyzed by ~11 nm-sized α-Mo_2C and ~16 nm-sized γ-Mo_2N nanoparticles synthesized by the 'urea glass route'. Both kinds of particles were demonstrated by X-ray diffraction, elemental analysis and transmission electron microscopy to be crystalline, single phase, homogeneous and defined in sizes. Hydrogen evolution was performed using these materials and also commercially available Mo_2C, MoB and Pt in 1M KOH and 0.5 M H_2SO_4 electrolytes. Among the non-noble metal catalysts studied, α-Mo_2C prepared by the urea glass route showed excellent HER performance especially in KOH electrolyte. At a catalyst loading of 102 μg cm^{-2}, a low overpotential (η) of 176 mV was needed to produce 10 mA cm^{-2} H_2. The corresponding turnover frequency is 0.5 s^{-1}. These figures of merit are highly favorable when compared with those exhibited by other non-precious metal HER catalysts. Online gas chromatography confirmed that only H_2 is formed. The as-synthesized Mo_2C and Mo_2N nanocatalysts showed negligible overpotential losses after undergoing

acceleration degradation tests in both acid and alkali. This is noteworthy since very few catalysts are active in these two extreme pHs.[11, 26, 27] We believe that the findings of this study will contribute significantly to the synthesis and development of highly- active and stable Mo-based electrocatalysts for hydrogen evolution.

2. Experimental

2.1. Synthesis of Molybdenum Carbides / Nitrides

The Mo_2C and Mo_2N were synthesized via our 'urea glass route'.[23] Ethanol was added to the solid metal precursor $MoCl_5$ to a concentration of 1.45M. $MoCl_5$ reacts with the alcohol to form Mo-orthoesters. Various quantities of solid urea were added to the alcoholic solution to give the desired urea/metal precursor molar ratio (R). The mixture was then stirred until the urea was completely solubilized (dissolution time depends on the ratio but usually is less than 1 h). In the presence of the metal precursors, solubility of urea is significantly higher than in pure ethanol (4.877 g / 100 g at 18.2 ^{o}C), indicating the formation of soluble complexes and coordination polymers. The gel-like precursors were then placed in crucibles and heated at 800 ^{o}C for 3 h (plus 4 h to reach the temperature) under N_2 gas flow. After calcinations, silvery-black powders were obtained. We were able to reproducibly prepare pure α-Mo_2C or γ-Mo_2N by simply changing the ratio R.

2.2. Physical and Chemical Characterization of the Catalysts

Elemental analysis of the as-synthesized molybdenum carbides / nitrides was performed using a Vario El Elementar. X-ray diffraction (XRD) of the films was performed on a Bruker D8 diffractometer using Cu-Kα radiation (λ = 0.154 nm) and a scintillation counter (or a KeveX Detector). The XRD patterns were identified based on comparisons with data from the ICDD-

PDF-4+ database. Transmission electron microscopy (TEM) was performed using a Zeiss EM 912Ω or JEOL TEM-3010 microscope. The acceleration voltages of the two instruments were 120 kV and 300 kV respectively. Samples were ground, suspended in ethanol and sonicated for 2 minutes in an ultrasonic bath. One drop of this suspension was put on a carbon-coated copper grid and left to dry in air. Surface area was determined by the Brunauer–Emmett–Teller (BET) method on a Micromeritics ASAP 2020 at 77 K. The samples were degassed at 363 K prior to N_2 sorption.

2.3. Electrochemical Measurements

The working electrodes were prepared as follows: A mixture of 2 mg Mo_2C or Mo_2N, 2 mg carbon black (Black Pearl 2000, Cabot Corp.), 800 μL Type I water (Barnstead Nanopure), 150 μL ethanol, and 50 μL Nafion solution (5% in a mixture of lower aliphatic alcohols and water, Aldrich) was ultrasonicated for 30 min to obtain a homogeneous ink. 10 μL catalyst ink was dropped onto a 5 mm diameter glassy carbon (GC) RDE (0.196 cm^2 geometrical area, Pine Instrument) and dried at room temperature. The resulting catalyst loading was 102 μg cm^{-2}. For comparison, electrodes comprised of commercial Pt/C (20 % Pt on Vulcan XC 72, Premetek Co.), commercial c-Mo_2C (99%, GoodFellow Inc.) and molybdenum boride (c-MoB, 99.5%, Aldrich) catalyst were also prepared. For Pt/C sample, 5 μL of catalyst ink (2 mg mL^{-1} Pt/C catalyst) was dropped onto the GC RDE electrode resulting in a catalyst loading of 51 μg cm^{-2}. The geometric surface area of the glassy carbon electrode was used for calculating the current densities reported in this work.

Electrochemical measurements were performed in a conventional three-electrode glass cell at 298 K using a bipotentiostat (Pine Instrument) equipped with a rotating disk electrode (RDE). A graphite rod was used as the counter electrode. $Hg/HgSO_4$, K_2SO_4 (saturated) and

Hg/HgO, KOH (1 M) were used as reference electrodes in acidic and alkaline media, respectively. All the potentials are reported with respect to the reversible hydrogen electrode (RHE). The electrolytes were purged with N_2 for 15 min prior to the measurements to remove dissolved oxygen. During the test, the headspace of the electrochemical cell was purged with N_2. The electrocatalytic activities of the catalysts were measured by linear sweep voltammetry (LSV) at a scan rate of 2 mV s^{-1} with a rotation speed of 900 rpm.

Electrochemical impedance spectroscopy (EIS) was carried out using an Autolab PGSTAT 30 potentiostat (Eco Chemie, Netherlands). Experiment EIS data were analyzed and fitted with the software ZView.

3. Results and Discussion

3.1. Controllable Formation and Characterization of Molybdenum Carbides/Nitrides

Successful preparation of high purity Mo carbide or Mo nitride particles was confirmed by both X-ray diffraction and elemental analysis of the as-synthesized powders (Figure 1a and Table 1). For R=7, peaks can be assigned to the plane (100), (002), (101), (102), (110), (103), (112) and (201) of α-Mo_2C (ICDD 00-035-0787). For R=1, the diffraction peaks of the sample can be assigned to the plane (111), (200), (220), (311) and (222) of γ-Mo_2N (ICDD 00-025-1366). No other crystalline side phases (for example, from MoO_x or Mo metal) could be observed in either of the XRD patterns. The purity of the samples especially from amorphous or graphitized carbon is also demonstrated by the absence of carbon signals at 2θ=21-26^o in the XRD patterns.[28] Elemental analysis of the α-Mo_2C and γ-Mo_2N corroborate the above results by measuring C and N content that are very close to their respective theoretical values (Table 1).

Using the Scherrer equation on multiple XRD peaks, the average sizes of the Mo_2C and Mo_2N catalysts were calculated to be ~11 and ~16 nm respectively.

The sizes of the catalysts were imaged by TEM (Figures 1b and c, Supplementary Information S1). The Mo_2C and Mo_2N were in the form of nanoparticles with respective sizes of 2-17 and 5-25 nm. These dimensions are in good agreement with estimations made by the use of the Scherrer equation (~11 nm for Mo_2C, ~16 nm for Mo_2N). High resolution TEM of the catalysts further corroborates the crystallinity of the particles (Supplementary Information S1). The BET surface areas of the Mo_2C and Mo_2N catalysts were 9.1 and 9.8 m^2/g respectively.

3.2. Electrochemical Hydrogen Evolution Reaction

The polarization curves and corresponding Tafel slopes of the as-synthesized α-Mo_2C and γ-Mo_2N, as well as reference electrocatalysts, in 1 M KOH or 0.5 M H_2SO_4 are presented in Figure 2. α-Mo_2C is highly efficacious for HER especially in 1 M KOH, with an onset potential of ~-100 mV, beyond which the cathodic current increases rapidly. This onset potential is significantly less negative than those of commercial c-Mo_2C and c-MoB catalyst, which are -160 and -210 mV respectively.[10] γ-Mo_2N, however, exhibits a more negative onset potential of ~-240 mV. Control experiments with only BP-2000 show that it is not catalytically active towards HER. Thus, all the measured HER current can be attributed to catalysis by the Mo-based nanoparticles. To compare the HER activities exhibited by the different catalysts, the overpotentials (η_{10}) needed to drive a current density of 10 mA cm^{-2} was selected as a reference. For α-Mo_2C, a η_{10} of 176 mV was required to produce 10 mA cm^{-2} in KOH, which is ~100 mV higher overpotential than Pt/C. In contrast, c-Mo_2C, c-MoB and γ-Mo_2N exhibited larger η_{10} values of 293 mV, 300 mV and 353 mV in alkaline media. It is significant that only small quantities of catalysts

(loading=0.102 mg cm^{-2}) were required to achieve these measured currents. Online gas chromatography was used to probe the gas compounds formed at -0.25 and -0.35 V (Supplementary Information S2). Only H_2 gas was detected, and all the cathodic currents were utilized for its production (~100% current efficiency).

The turnover frequencies (TOF) of H_2 evolution per surface Mo atom were evaluated (Supplementary Information S3). The number of sites present were estimated by considering the average sizes of these nanoparticles as determined by the Scherrer equation, and approximating their shapes to spherical. All sites were assumed to be catalytically-active. Mo_2C catalyzed hydrogen evolution in KOH electrolyte with TOFs of 0.5, 0.9 and 2.5 s^{-1} at η= 176, 200 and 250 mV respectively. Mo_2N catalyzed HER in KOH with TOFs of 0.07 and 0.7 s^{-1} at η=250 mV and 352 mV. These values are compared with those exhibited by several non-precious metal HER catalysts and presented in Table 2.[6-10, 12, 13, 16, 25, 29-33] The representative TOF values of other catalysts are: 0.36 and 0.50 s^{-1} for Ni-Mo and Ni_2P respectively (η= 200 mV), 3 s^{-1} for molecular $Mo_3S_{13}^{2-}$ (η=200 mV), and 0.19-0.86 s^{-1} for Mo_xC coated on Ni foam (η= 250 mV). Thus, the remarkable HER activities of our Mo_2C nanoparticles are higher than many other cost-effective electrocatalysts reported to date. It is noteworthy that this is achievable even though the catalysts are only physically mixed with carbon black. Chemical immobilization of the catalysts onto carbon supports (previously shown to aid in the catalytic activity of Mo_2C) or doping with other elements were not necessary.

Tafel plots, which reflect the reaction mechanism of HER on Mo_2C and Mo_2N catalysts, are presented in Figures 2b and d. HER using Mo_2C nanocatalysts exhibit a Tafel slope of 58 and 56 mV dec^{-1} in KOH and H_2SO_4 electrolytes. This suggests that hydrogen evolution on the Mo_2C

go through a Heyrovsky-Volmer mechanism with the Heyrovsky step as the rate determining step.[34] Carbon supported Mo_2C and nanoporous Mo_2C nanowires also exhibit similar Tafel slopes for HER.[7, 35] On the other hand, commercial c-Mo_2C catalyst exhibits a larger Tafel slope of ~100 mV dec^{-1}. We believe that this disparity could be attributed to the sizes of the Mo_2C catalysts. The average grain size of c-Mo_2C was ~125 nm, which is significantly larger than the ~11 nm Mo_2C synthesized via the urea glass route. Tafel slope values exhibited by Mo_2C for HER have also previously observed to increase with the size of the particles.[7, 10] Mo_2N nanocatalysts showed a Tafel slope of ~100 mV dec^{-1} in both acid and alkali, indicating that the Volmer reaction would be slower on these catalysts than on Mo_2C. It is noteworthy that similar Tafel slopes are observed in both KOH and H_2SO_4 using either Mo_2C or Mo_2N, suggesting that the same reaction mechanism transpired for HER in these two electrolytes (in contrast with Pt/C).

These results were corroborated by electrochemical impedance spectroscopy (EIS) performed from 100 kHz to 0.1 Hz at selected overpotential values with amplitude of 5 mV. Representative Nyquist and corresponding Bode plots of Mo_2C in KOH electrolytes are shown in Figures 3a and b. A two-time constant model, which consists of solution resistance (R_s) in series with two parallel constant phase element – resistance (CPE-R) elements, fits the experiment data well at all the overpotentials tested (Figure S4).[36] Two semicircles on Nyquist plot are exhibited, with the higher frequency one related to the surface porosity, while the lower frequency one related to the charge transfer process of hydrogen evolution. The charge transfer resistance (R_{ct}) of HER on the Mo_2C decreases with the overpotential, from 1377 Ω at a η=100 mV to 32.9 Ω at η=200 mV. To reflect purely the charge transfer kinetic of HER on the Mo_2C, the Tafel slope was obtained from a plot of log (R_{ct}^{-1}) versus overpotential from the EIS data, as shown in Figure 3c. The Tafel slope is calculated to be 57 mV dec^{-1}, which is the same as that obtained from the

LSV data in Figure 2 (Table S2). This shows that the contribution of mass-transfer resistance is negligible under the RDE test configuration. Figure 3d compares the Nyquist plots of Mo_2C and Mo_2N at overpotentials of 200 and 300 mV respectively. Mo_2C exhibits lower charge transfer resistance and hence higher catalytic activity for HER than Mo_2N, as shown by its lower R_{ct} values. In acidic media, similar EIS behaviors are observed (Figure S5). Thus consistent with the LSV results, EIS demonstrates that rapid electron transfers happen on the Mo_2C for HER, and confirms that Mo_2C exhibits higher activities towards HER in alkali than in acid (Figure S6).

3.3. Acceleration Degradation Tests in KOH and H_2SO_4

To assess the long-term durability of the catalysts for HER, the LSV curve of the electrodes were measured at 2 mV s^{-1} in KOH and H_2SO_4 electrolytes (Figure 4). The electrodes were then subjected to continuous potential cycling for 1000 cycles at 100 mV s^{-1}. The scan potentials were from 0.2 to -0.3 V for the Mo_2C, and 0.2 to -0.4 V for the Mo_2N, respectively. The lower-bound (negative) potentials were selected in order to ensure significant production of H_2 at current densities of at least -70 mA cm^{-2} (a less cathodic potential was needed for Mo_2C as it is more reactive than Mo_2N). The vigorous production of H_2 bubbles is also a mean to probe the mechanical stability of the catalyst film- glassy carbon electrode ensemble. The upper-bound potential was kept below 0.2 V in order to prevent any oxidation of the Mo_2C and Mo_2N. Polarization curves of the catalysts were subsequently recorded in fresh electrolytes (Figure 4). Mo_2C and Mo_2N showed excellent stability for HER in both acid and alkali, as demonstrated by the negligible loss of current at the low overpotential region. The Tafel slopes exhibited by Mo_2C and Mo_2N remain constant at ~58 and ~100 mV/dec respectively, which demonstrate that the HER mechanism is unaltered by potential cycling of the catalysts. XRD of the catalysts prior to and after the durability tests also revealed reflections belonging to the pure compounds, i.e., α-

Mo_2C or γ-Mo_2N (Figure 5). No changes in the structure of the catalysts could be detected after HER, which further confirm their stability.

The high HER activity and stability exhibited by the α-Mo_2C nanoparticles in acid and alkali is noteworthy, since very few catalysts are active in electrolytes with such extreme pHs.[11, 26, 27] We attribute its excellent catalytic activity to its smaller particle size which will facilitate facile electron transfer for HER. The trace amount of nitrogen atoms in the α-Mo_2C could also synergistically interact with the Mo centers and hence enhance its activity for HER (Table 1). Similar effects have been proposed for a β-Mo_2C/γ-Mo_2N composite (MoSoy) that exhibited better HER activity as compared to a simple physical mixture of Mo_2C and Mo_2N.[16] The nature of the synergy during HER such as extent of charge transfers between the N and/or C atoms with the Mo atoms would have to be probe with in situ X-ray absorption spectroscopy.[37] Dispersing the α-Mo_2C in BP-2000 will also improve the conductivity of the entire catalyst film, and increase the contact between the catalyst and aqueous electrolyte. Our approach of physically mixing Mo_2C or Mo_2N with carbon black is easier than having to chemically bond them onto carbon supports, but still yield catalyst films that are highly active.[7, 25] We believe that the findings of this study will contribute significantly to the development of highly-active Mo-based electrocatalysts for industrial-scale water splitting.

4. Conclusions

α-Mo_2C and γ-Mo_2N nanoparticles, which are targeted for catalyzing HER, have been synthesized by a urea glass route. Hydrogen evolution was performed in both 1M KOH and 0.5 M H_2SO_4 electrolytes. The as-prepared Mo_2C showed exceptional catalytic activity towards HER. At a catalyst loading of 102 μg cm^{-2}, only a low overpotential of 176 mV was needed to produce

10 mA cm^{-2} of H_2 (TOF: 0.5 s^{-1}) in KOH electrolyte. Online gas chromatography demonstrates that the reaction proceeds at ~100% current efficiency. Both catalysts exhibited negligible overpotential losses after durability tests in acid and alkali. Our studies show that Mo_2C nanoparticles synthesized by the urea glass route is one of the most efficacious HER catalysts made of earth abundant materials, and would be a promising replacement for platinum in the alkaline water electrolyzer.

Acknowledgements

This work is financially supported by a start-up grant (R143-000-515-133) from the National University of Singapore and the Max Planck Society. The authors kindly thank Drs. Guylhaine Clavel and Chung Shou Chen for the TEM measurements.

References

1. N. S. Lewis and D. G. Nocera, *Proc. Natl. Acad. Sci.*, 2006, **103**, 15729-15735.
2. N. Armaroli and V. Balzani, *ChemSusChem*, 2011, **4**, 21-36.
3. C. G. Morales-Guio, L.-A. Stern and X. Hu, *Chem. Soc. Rev.*, 2014, **43**, 6555-6569.
4. B. E. Conway and G. Jerkiewicz, *Electrochim. Acta*, 2000, **45**, 4075-4083.
5. S. Trasatti, *J. Electroanal. Chem.*, 1972, **39**, 163-184.
6. C. Wan, Y. N. Regmi and B. M. Leonard, *Angew. Chem. Int. Ed.*, 2014, **53**, 6407-6410.
7. W. F. Chen, C. H. Wang, K. Sasaki, N. Marinkovic, W. Xu, J. T. Muckerman, Y. Zhu and R. R. Adzic, *Energy Environ. Sci.*, 2013, **6**, 943-951.
8. W. F. Chen, K. Sasaki, C. Ma, A. I. Frenkel, N. Marinkovic, J. T. Muckerman, Y. M. Zhu and R. R. Adzic, *Angew. Chem. Int. Ed.*, 2012, **51**, 6131-6135.

9. B. F. Cao, G. M. Veith, J. C. Neuefeind, R. R. Adzic and P. G. Khalifah, *J. Am. Chem. Soc.*, 2013, **135**, 19186-19192.

10. H. Vrubel and X. L. Hu, *Angew. Chem. Int. Ed.*, 2012, **51**, 12703-12706.

11. W. F. Chen, J. T. Muckerman and E. Fujita, *Chem. Comm.*, 2013, **49**, 8896-8909.

12. J. Zhang, X. Meng, J. Zhao and Z. Zhu, *ChemCatChem*, 2014, **6**, 2059-2064.

13. C. Ge, P. Jiang, W. Cui, Z. Pu, Z. Xing, A. M. Asiri, A. Y. Obaid, X. Sun and J. Tian, *Electrochim. Acta*, 2014, **134**, 182-186.

14. S. Wirth, F. Harnisch, M. Weinmann and U. Schroder, *Appl. Catal. B*, 2012, **126**, 225-230.

15. N. S. Alhajri, D. H. Anjum and K. Takanabe, *J. Mater. Chem. A*, 2014, **2**, 10548-10556.

16. W.-F. Chen, S. Iyer, S. Iyer, K. Sasaki, C.-H. Wang, Y. Zhu, J. T. Muckerman and E. Fujita, *Energy Environ. Sci.*, 2013, **6**, 1818-1826.

17. C. A. Wolden, A. Pickerell, T. Gawai, S. Parks, J. Hensley and J. D. Way, *ACS Appl. Mater. Interfaces*, 2011, **3**, 517-521.

18. J.-G. Choi, J. R. Brenner, C. W. Colling, B. G. Demczyk, J. L. Dunning and L. T. Thompson, *Catal. Today*, 1992, **15**, 201-222.

19. M. K. Kolel-Veetil, S. B. Qadri, M. Osofsky and T. M. Keller, *Chem. Mater.*, 2005, **17**, 6101-6107.

20. C. Giordano and M. Antonietti, *Nano Today*, 2011, **6**, 366-380.

21. S. T. Oyama, *Catal. Today*, 1992, **15**, 179-200.

22. Y. C. Kimmel, D. V. Esposito, R. W. Birkmire and J. G. G. Chen, *Int. J. Hydrogen Energy*, 2012, **37**, 3019-3024.

23. C. Giordano, C. Erpen, W. T. Yao and M. Antoniett, *Nano Lett.*, 2008, **8**, 4659-4663.

24. C. Giordano, C. Erpen, W. T. Yao, B. Milke and M. Antonietti, *Chem. Mater.*, 2009, **21**, 5136-5144.

25. D. H. Youn, S. Han, J. Y. Kim, J. Y. Kim, H. Park, S. H. Choi and J. S. Lee, *ACS Nano*, 2014, **8**, 5164-5173.

26. M. C. Weidman, D. V. Esposito, Y.-C. Hsu and J. G. Chen, *J. Power Sources*, 2012, **202**, 11-17.

27. J. R. McKone, S. C. Marinescu, B. S. Brunschwig, J. R. Winkler and H. B. Gray, *Chem. Sci.*, 2014, **5**, 865-878.

28. Z. Q. Li, C. J. Lu, Z. P. Xia, Y. Zhou and Z. Luo, *Carbon*, 2007, **45**, 1686-1695.

29. E. J. Popczun, J. R. McKone, C. G. Read, A. J. Biacchi, A. M. Wiltrout, N. S. Lewis and R. E. Schaak, *J. Am. Chem. Soc.*, 2013, **135**, 9267-9270.

30. J. Kibsgaard, T. F. Jaramillo and F. Besenbacher, *Nat. Chem.*, 2014, **6**, 248-253.

31. Y. Zhao, K. Kamiya, K. Hashimoto and S. Nakanishi, *Angew. Chem. Int. Ed.*, 2013, **52**, 13638-13641.

32. J. F. Xie, J. J. Zhang, S. Li, F. Grote, X. D. Zhang, H. Zhang, R. X. Wang, Y. Lei, B. C. Pan and Y. Xie, *J. Am. Chem. Soc.*, 2013, **135**, 17881-17888.

33. J. R. McKone, B. F. Sadtler, C. A. Werlang, N. S. Lewis and H. B. Gray, *ACS Catal.*, 2013, **3**, 166-169.

34. B. E. Conway and B. V. Tilak, *Electrochim. Acta*, 2002, **47**, 3571-3594.

35. L. Liao, S. N. Wang, J. J. Xiao, X. J. Bian, Y. H. Zhang, M. D. Scanlon, X. L. Hu, Y. Tang, B. H. Liu and H. H. Girault, *Energy Environ. Sci.*, 2014, **7**, 387-392.

36. B. Losiewicz, A. Budniok, E. Rowinski, E. Lagiewka and A. Lasia, *Int. J. Hydrogen Energy*, 2004, **29**, 145-157.

37. D. Friebel, M. Bajdich, B. S. Yeo, M. W. Louie, D. J. Miller, H. S. Casalongue, F. Mbuga, T.-C. Weng, D. Nordlund and D. Sokaras, *Phys. Chem. Chem. Phys.*, 2013, **15**, 17460-17467.

Figure Captions

Figure 1: (a) X-Ray diffraction patterns of Mo_2C and Mo_2N synthesized by the urea glass route. The expected patterns (vertical lines) are included for comparison. TEM images of the (b) Mo_2C and (c) Mo_2N nanoparticles.

Figure 2: (a) Polarization curves and (b) corresponding Tafel plots of Mo_2C, Mo_2N, Pt/C, commercial Mo_2C (c-Mo_2C) and commercial MoB (c-MoB) in N_2-saturated 1 M KOH with *iR* correction. (c) Polarization curves and (d) corresponding Tafel plots of Mo_2C, Mo_2N, Pt/C, commercial Mo_2C (c-Mo_2C) and commercial MoB (c-MoB) in N_2-saturated 0.5 M H_2SO_4 with iR correction. BP-2000: glassy carbon electrode loaded with BP-2000 only. Scan rate: 2 mV s^{-1}; rotating speed: 900 rpm.

Figure 3: (a) Nyquist and (b) corresponding Bode plots of Mo_2C recorded at selected overpotentials in N_2-saturated 1 M KOH. (c) Plots of log (R_{ct}^{-1}) vs overpotential for Mo_2C. (d) Comparison between the Nyquist plots of Mo_2C at an overpotential of 200 mV and that of Mo_2N at an overpotential of 300 mV.

Figure 4: Durability test of Mo_2C and Mo_2N electrodes with an initial LSV polarization curve (dashed) and after 1000 cycles (solid) in (a) 1 M KOH and (b) 0.5 M H_2SO_4 solution without *iR* correction. Scan rate: 2 mV s^{-1}; rotating speed: 900 rpm.

Figure 5: XRD patterns of (a) Mo_2C and (b) Mo_2N catalysts before and after the durability test in N_2-saturated 1 M KOH and N_2-saturated 0.5 M H_2SO_4. The expected patterns (vertical lines) are included for comparison.

Sample	Metal Precursor	R	N (wt %)	C (wt %)
α-Mo_2C	$MoCl_5$	7	0.86	5.35 (5.8)
γ-Mo_2N	$MoCl_5$	1	7.26 (6.8)	0.17

Table 1: Experimental details and elemental analysis of α-Mo_2C and γ-Mo_2N synthesized via the urea glass route. The theoretical amount of C and N in α-Mo_2C and γ-Mo_2N are presented respectively in parenthesis next to their experimental values.

Catalyst	Loading (mg cm^{-2})	Electrolyte	Current Density (mA cm^{-2})	η (mV)	Turnover Frequency for H_2 Production[b]
α-Mo_2C[a]	0.102	0.5 M H_2SO_4	10	198	0.5 s^{-1} (η=200 mV, I = -10 mA cm^{-2})
		1 M KOH		176	0.5 s^{-1} (η=176 mV, I = -10 mA cm^{-2}) 0.9 s^{-1} (η=200 mV, I = -19.5 mA cm^{-2}) 2.5 s^{-1} (η=250 mV, I = -54.9 mA cm^{-2})
γ-Mo_2N[a]	0.102	0.5 M H_2SO_4	10	381	0.03 s^{-1} (η=250 mV, I = -0.47 mA cm^{-2}) 0.7 s^{-1} (η=381 mV, I = -10 mA cm^{-2})
		1 M KOH		353	0.07 s^{-1} (η=250 mV, I = -0.94 mA cm^{-2}) 0.7 s^{-1} (η=352 mV, I = -10 mA cm^{-2})
Mo_2C[10]	1.4	1 M H_2SO_4	10	~210	-
	0.8	1 M KOH	10	~190	-
β-Mo_2C[6]	0.28	0.1 M $HClO_4$	~3	~250	-
Mo_2C-carbon nanocomposites[15]	0.25	0.05 M H_2SO_4	5	~265	-
Mo_2C nanowires[13]	0.357	0.5 M H_2SO_4	10.2	200	-
Mo_2C/CNT[7]	2	0.1 M $HClO_4$	10	152	-
Mo_xC/Ni[12]	N.A.	0.5 M H_2SO_4	10	~150	0.86 s^{-1} (η=250 mV, I = -34.7mA cm^{-2})
Mo_2C/GR[25]	0.65-0.67	0.5 M H_2SO_4	10	242	-
Mo_2C/CNT-GR[25]	0.65	0.5 M H_2SO_4	10	130	-
Mo_2N/CNT-GR[25]	0.67	0.5 M H_2SO_4	10	186	-
γ-Mo_2N[16]	2	0.1 M $HClO_4$	10	~300	-
$Co_{0.6}Mo_{1.4}N_2$[9]	0.24	0.1 M $HClO_4$	10	200	-
$NiMoN_x/C$[8]	0.25	0.1 M $HClO_4$	5	~220	-
NiMo[33]	0.1	2 M KOH	13.1	200	0.05s^{-1} (η=100 mV, I=2.0 mA cm^{-2}) 0.36s^{-1} (η=200 mV, I=13.1 mA cm^{-2})
	3	0.5 M H_2SO_4	20	80	-
Ni_2P[29]	1	0.5 M H_2SO_4	20	130	0.015s^{-1} (η=100 mV, I = -3.16mA cm^{-2}) 0.50s^{-1} (η=200 mV, I = -105mA cm^{-2})
$[Mo_3S_{13}]^{2-}$[30]	0.1	0.5 M H_2SO_4	10	180	3 s^{-1} (η=200 mV)
Oxygen-incorporated MoS_2[32]	0.285	0.5 M H_2SO_4	10	160-220	-
Fe-WCN[31]	0.4	H_2SO_4 + 0.5 M $NaSO_4$ (pH=1)	10	220	-

Table 2: Comparison of HER catalysts. η: overpotential required to achieve stated current density, CNT: carbon nanotubes, GR: graphene. [a]: this work; [b]: The TOFs of selected HER

catalysts are included for comparison. The applied overpotential and measured current are shown next to the TOF value.

Ma, et al. Figure 1

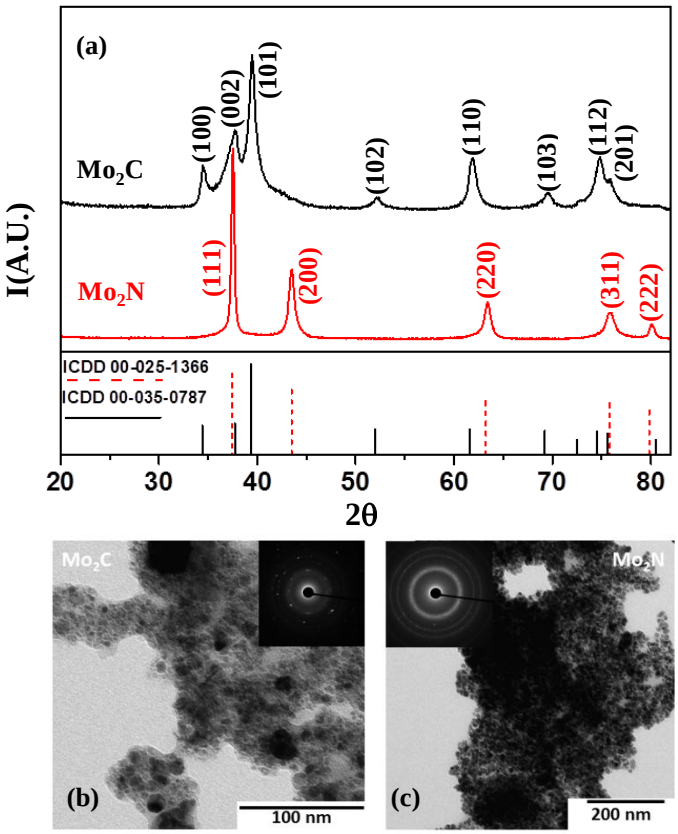

Figure 1: (a) X-Ray diffraction patterns of Mo_2C and Mo_2N synthesized by the urea-glass route. The expected patterns (vertical lines) are included for comparison. TEM images of (b) Mo_2C and (c) Mo_2N nanoparticles.

Ma, et al. Figure 2

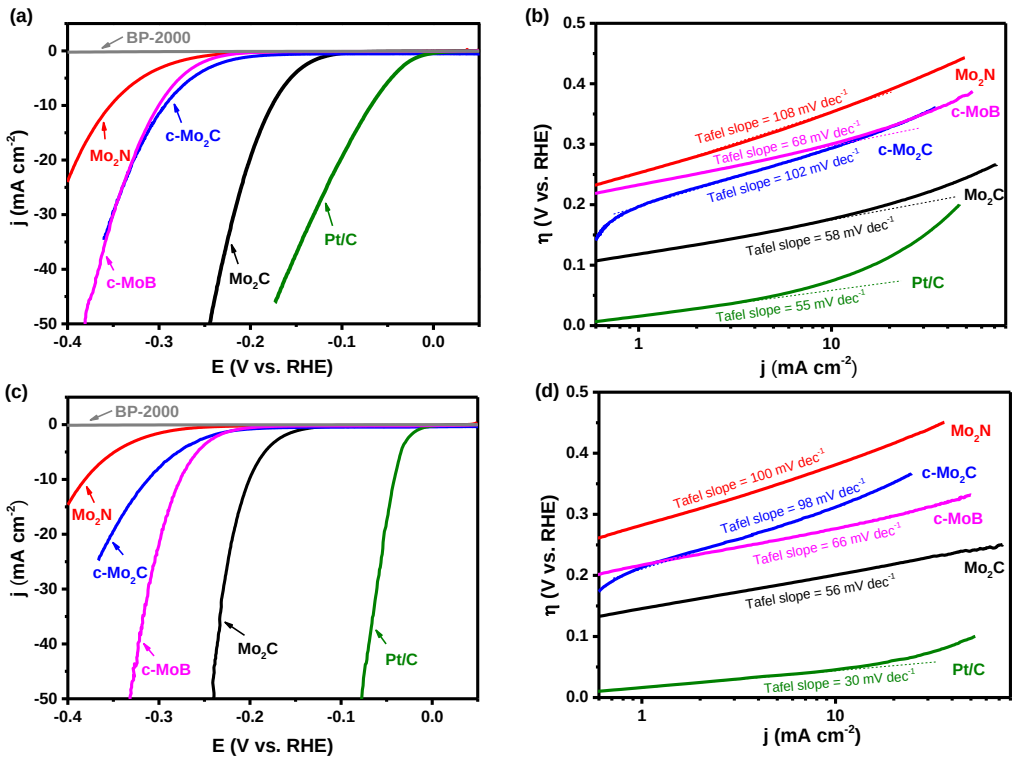

Figure 2: (a) Polarization curves and (b) corresponding Tafel plots of Mo_2C, Mo_2N, Pt/C, commercial Mo_2C (c-Mo_2C) and commercial MoB (c-MoB) in N_2-saturated 1 M KOH with iR correction. (c) Polarization curves and (d) corresponding Tafel plots of Mo_2C, Mo_2N, Pt/C, commercial Mo_2C (c-Mo_2C) and commercial MoB (c-MoB) in N_2-saturated 0.5 M H_2SO_4 with iR correction. BP-2000: glassy carbon electrode loaded with BP-2000 only. Scan rate: 2 mV s^{-1}; rotating speed: 900 rpm.

Ma, et al. Figure 3

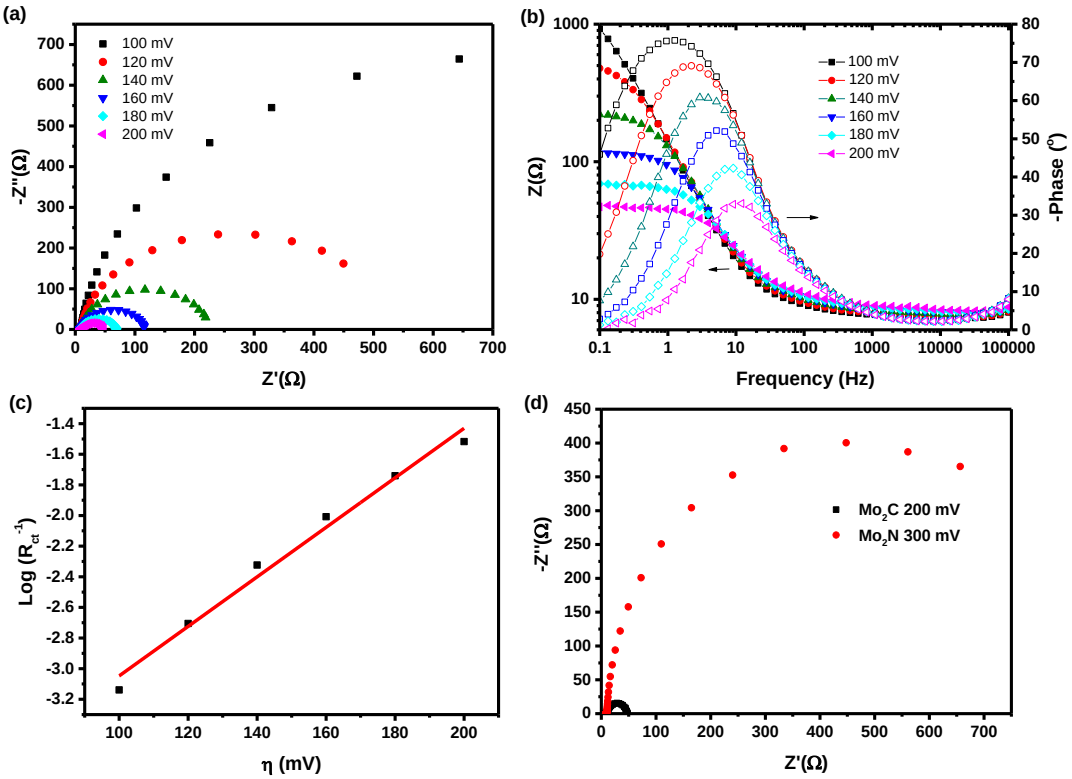

Figure 3: (a) Nyquist and (b) corresponding Bode plots of Mo_2C recorded at selected overpotentials in N_2-saturated 1 M KOH. (c) Plots of log (R_{ct}^{-1}) vs overpotential for Mo_2C. (d) Comparison between the Nyquist plots of Mo_2C at an overpotential of 200 mV and that of Mo_2N at an overpotential of 300 mV.

Ma, et al. Figure 4

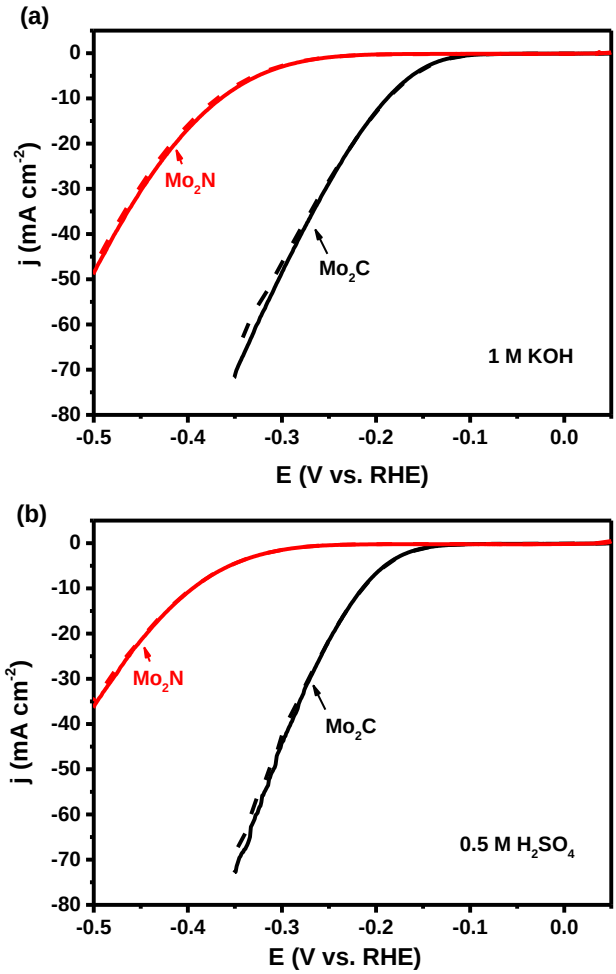

Figure 4: Durability test of Mo_2C and Mo_2N electrodes with an initial LSV polarization curve (dashed) and after 1000 cycles (solid) in (a) 1 M KOH and (b) 0.5 M H_2SO_4 solution without *iR* correction. Scan rate: 2 mV s^{-1}; rotating speed: 900 rpm.

Ma, et al. Figure 5

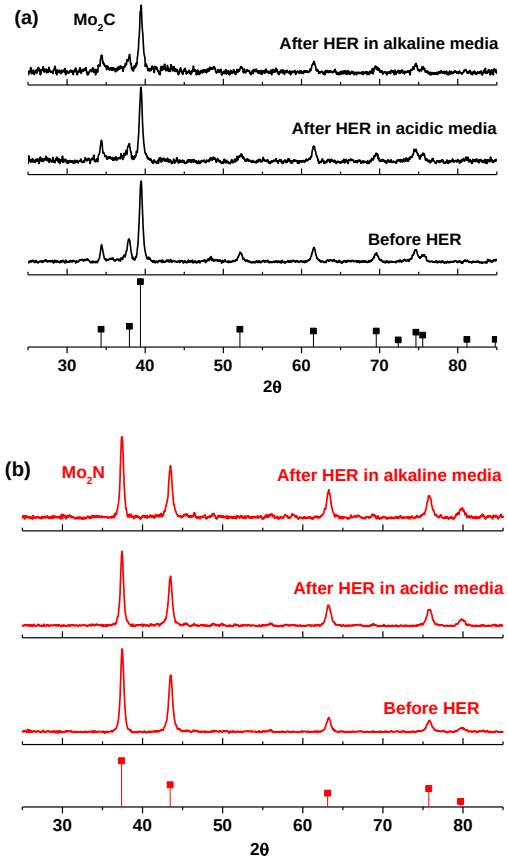

Figure 5: XRD patterns of (a) Mo_2C and (b) Mo_2N catalysts before and after the durability test in N_2-saturated 1 M KOH and N_2-saturated 0.5 M H_2SO_4. The expected patterns (vertical lines) are included for comparison.